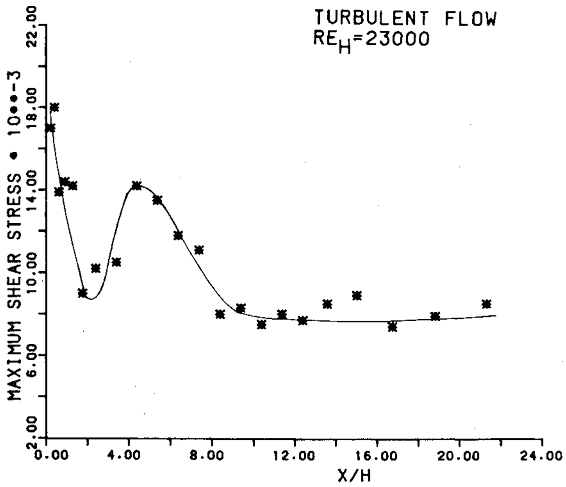

Fig. 3 Comptued distribution of maximum shear stress.

22.6×10^6 in that of Viswanath et al. Second, we consider a flat plate at zero thickness whereas Viswanath et al. consider a 6.25 deg wedge. The effect of the flat plate or the wedge is more pronounced near the trailing edge and attenuates downstream of the trailing edge.

It is also likely that the streamwise gradient of the normal stress, which is ignored in the eddy viscosity formulation, is contributing to lack of agreement. The streamwise gradient of the normal stress rapidly diminishes downstream of the trailing edge.

Viswanath et al. have also computed the flow past a flat plate utilizing a two-equation model of turbulence. Their computed results show good agreement with the experimental results, thus indicating that our results also are in accordance with the computations of the two-equation model.

For the far wake (not studied by Viswanath et al.) our computational results closely match the experimental results of Chevray and Kovasznay[5]; for example, the computed velocity defects at $x/\theta_0 = 258$ and 414 are 0.14 and 0.11 vs 0.17 and 0.11 measured by Chevray and Kovasznay.

Flow Past a Backward-Facing Step

This flow was computed for a step-height Reynolds number, $Re_H = 23{,}000$, and for a step height to inlet boundary-layer thickness of 1.0. The computed wall pressure distribution is shown in Fig. 2 and it demonstrates good qualitative agreement with that obtained experimentally by Chandrasuda and Bradshaw.[6] The maximum shear stress profile (Fig. 3) also exhibits good qualitative agreement with those of experiments considered in Ref. 7. The peak value computed near reattachment is 14×10^{-3}, compared to 11×10^{-3} measured in experiments. In contrast, most of the computations reported in Ref. 7, utilizing differential equation models, substantially overpredict the maximum shear stress.

One of the important features of a flow over a backward-facing step is the length of the separation bubble which was found to be 5.5 step heights in close agreement with the previous experimental studies.[8] This may be contrasted with the differential equation models of turbulence which are reported to considerably underpredict the length of the separation bubble.[7]

Reattachment and the subsequent development of the subboundary layer are other important features of the flow. In the present computations the maximum skin friction coefficient after reattachment is 1×10^{-3} vs 3×10^{-3} upstream of the corner. The skin friction distribution and, hence, the velocity distribution close to the wall and downstream of reattachment are underpredicted. This has also been the observation with the two-equation models although they are better than the eddy viscosity models in this regard.[9]

Conclusions

Our study indicates that eddy viscosity models can compute most features of a wake flow and a separated flow satisfactorily. The main drawback is their inability to predict accurately the shear stress close to the wall downstream of reattachment. This drawback seems to be shared with two-equation models, such as the k-ϵ model.

Acknowledgments

The authors are grateful to the Australian Research Grants Scheme for their continued financial support. Thanks are also due to Dr. David Wood for his comments on an earlier version of this manuscript.

References

[1]Srinivas, K. and Fletcher, C.A.J., "Finite Element Solutions for Laminar and Turbulent Flow," *International Journal of Numerical Methods for Fluids*, to appear, 1984.

[2]Fletcher, C.A.J., "On an Alternating Direction Implicit Finite Element Method for Fluid Flow Problems," *Computational Methods in Applied Mechanical Engineering*, Vol. 30, 1982, pp. 307-322.

[3]Deiwert, G. S., "Computation of Separated Transonic Turbulent Flows," *AIAA Journal*, Vol. 14, June 1976, pp. 735-740.

[4]Viswanath, P. R., Clearly, J. W., Seegmiller, H. L., and Horstman, C. C., "Trailing-Edge Flows at High Reynolds Number," AIAA Paper 79-1503, 1979.

[5]Chevray, R. and Kovasznay, L.S.G., "Turbulence Measurements in the Wake of a Thin Flat Plate," *AIAA Journal*, Vol. 7, Aug. 1969, pp. 1641-1643.

[6]Chandrasuda, C. and Bradshaw, P., "Turbulence Structure of a Reattaching Mixing Layer," *Journal of Fluid Mechanics*, Vol. 110, Sept. 1981, pp. 171-194.

[7]1980-1981 AFOSR-HTTM-Stanford Conference on Complex Turbulent Flows.

[8]Durst, F. and Tropea, C., "Turbulent, Backward-Facing Step Flows in Two-Dimensional Ducts and Channels," *Third International Symposium on Turbulent Shear Flows*, University of California, Davis, 1981, pp. 18.1-18.6.

[9]Horstman, C. C., Settles, G. S., Williams, D. R., and Bogdonoff, S. M., "A Reattaching Free Shear Layer in Compressible Turbulent Flow," *AIAA Journal*, Vol. 20, Jan. 1982, pp. 79-85.

Nonequilibrium Arc Modeling

J. Pantuso Sudano*
Instituto Tecnológico de Aeronáutica,
São Jose dos Campos, Brazil

MANY attempts have been made to derive models that describe the thermal and electrical characteristics of arc behavior.[1] Elenbaas and Heller[2] first attempted to solve the conservative equations for an arc column. They considered an arc column in any asymptotic equilibrium flow regime which leads to a decoupling of the energy and momentum equations. Using the energy conservation equation plus Fourier's law of heat conduction they obtained the Elenbaas-Heller equation. Several authors[3] have presented solutions of the Elenbaas-Heller equation both for constant and temperature-dependent transport coefficients., These solutions allow the determination of the local physical parameters of the plasma and their relation to the external energy input and to the dimensional characteristics of the arc. This information is useful in practical arc design. In many technical applications

Received March 18, 1983. Copyright © American Institute of Aeronautics and Astronautics, Inc., 1983. All rights reserved.

*Department of Physics.

involving arc discharges, the production of a given temperature distribution is required to suit some special purpose.

In this Note, a modified Elenbaas-Heller equation is written in the frame of nonequilibrium thermodynamics. If the state of nonequilibrium of the plasma is near a state of equilibrium, it can be assumed that the plasma is in a state of local thermodynamic equilibrium. However, it is precisely in the frame of local thermodynamic equilibrium that nonequilibrium thermodynamics applies. It follows that instead of using the simple Fourier law of heat conduction a generalized phenomenological equation must be used in conjunction with the energy conservation equation. This work treats precisely this subject.

Neglecting radiation and magnetic fields effects from the arc entirely, the energy balance equation may be written as[4]

$$\operatorname{div} \boldsymbol{W} = \boldsymbol{J} \cdot \boldsymbol{E} \tag{1}$$

where, according to nonequilibrium thermodynamics,[4]

$$\boldsymbol{W} = -\beta \boldsymbol{E}' - k \nabla T \tag{2}$$

$$\boldsymbol{E}' = \boldsymbol{E} + (1/en_e) \nabla p_e \tag{3}$$

$$\boldsymbol{J} = \sigma \boldsymbol{E}' + \alpha \nabla T \tag{4}$$

where $\boldsymbol{W}$ is the heat flow vector, $\boldsymbol{E}'$ a generalized electric field, T the plasma temperature, $\boldsymbol{E}$ the electric field, n_e the electron number density, p_e electron pressure, σ the electrical conductivity, K the thermal conductivity, β a transport coefficient called the coefficient for electron energy flow due to electric field,[5] and α^{-1} is the thermoelectric power.[5]

From Eqs. (2-4) one can verify the occurrence, in general, of interference or cross phenomena; in this case, heat flow due to an electric field and electricity flow due to temperature gradient. Combine Eqs. (2-4) results in

$$\boldsymbol{W} = -\beta \boldsymbol{E} - K' \nabla T \tag{5}$$

$$\boldsymbol{J} = \sigma \boldsymbol{E} + \alpha' \nabla T \tag{6}$$

where

$$K' = (\beta k_B / e) + k \tag{7}$$

$$\alpha' = (\sigma k_B / e) + \alpha \tag{8}$$

The equation of state

$$p_e = n_e k_B T \tag{9}$$

was used to eliminate p_e with the additional assumption that the electron number density n_e is constant.

The Elenbaas-Heller equaton according nonequilibrium thermodynamics is written by substituting $\boldsymbol{W}$ and $\boldsymbol{J}$ given by Eqs. (5) and (6) in Eq. (1) this results in

$$\operatorname{div}(-\beta \boldsymbol{E} - k' \nabla T) = (\sigma \boldsymbol{E} + \alpha' \nabla T) \cdot \boldsymbol{E} \tag{10}$$

The solution of this equation is generally a difficult problem because the transport coefficients β, k', σ, α' are usually temperature dependent, which makes Eq. (10) nonlinear or quasilinear. This Note is limited to the presentation of an analytical solution, for the case of constant transport coefficients, that can be used to guide numerical modeling and gives a feeling of the effects of cross phenomena. In cylindrical coordinates r, ϕ, z and with axial symmetry, Eq. (10) becomes

$$\frac{\partial^2 T}{\partial r^2} + \frac{1}{r}\frac{\partial T}{\partial r} + \frac{\partial^2 T}{\partial z^2} + \frac{\alpha'}{k'} E_z \frac{\partial T}{\partial z} + \frac{\sigma}{k'} E_z^2 = 0 \tag{11}$$

where E_z is the constant applied electric field strength along the axis. In general, this electric field is given by

$$\boldsymbol{E} = -\frac{1}{c}\frac{\partial A}{\partial t} - \nabla \psi \tag{12}$$

The magnetic field and polarization effects are neglected entirely herein. The electric field $\boldsymbol{E}$ is the applied external field which we assume to be constant. Equation (11) is a nonhomogeneous linear partial differential equation. The heat source term is $(\sigma/k')E_z^2$. It is desirable to solve the preceding differential equation subject to the following type of boundary condition which is called standard second kind one.[6] The normal derivate of the temperature is specified along a boundary surface

$$\frac{\partial T}{\partial n} = f(r_s) \tag{13}$$

where r_s is on the boundary surface, $\partial/\partial n$ represents differentiation along the outward normal to the surface.

Applying this boundary condition assume that the heat flux $\boldsymbol{W}$ at the boundary of the plasma column is constant and independent of z. Then the temperature distribution must be of the form

$$T(r,z) = Az + g(r) \tag{14}$$

where the boundary condition ($W_B = \text{const}$) is the same as

$$\left(\frac{\partial T}{\partial r}\right)_{r=R_c} = \left(\frac{\mathrm{d}g}{\mathrm{d}r}\right)_{r=R_c} = \text{const} \tag{15}$$

since by Eq. (5)

$$W = -\beta E - k' \nabla T \tag{16}$$

In our case β and E are constants. Substitution of Eq. (14) into Eq. (11) leads to the following relationship:

$$\frac{\mathrm{d}^2 g}{\mathrm{d}r^2} + \frac{1}{r}\frac{\mathrm{d}T}{\mathrm{d}r} + m^2 = 0 \tag{17}$$

where

$$m^2 = \frac{E_z}{k'}(A\alpha' + \sigma E_z) \tag{18}$$

The solution of Eq. (17) may be obtained from the addition of a solution g_h of the homogeneous equation

$$\frac{\mathrm{d}^2 g}{\mathrm{d}r^2} + \frac{1}{r}\frac{\mathrm{d}g}{\mathrm{d}r} = 0 \tag{19}$$

plus a particular solution of the inhomogeneous equation (17).

The solution of the homogeneous equation (19) is:

$$g_h = T_a + C \log r \tag{20}$$

where T_a and C are integration constants. The term $C \log r$ is divergent for $r = 0$ and is not taken into account. Then,

$$g_h = T_a \tag{21}$$

The particular solution of the inhomogeneous equation is

$$g_p = -\frac{E_z}{4k'}(\alpha' A + \sigma E_z) r^2 \tag{22}$$

Then the solution of Eq. (17) is

$$g(r) = T_a - \frac{E_z}{4k'}(\alpha' A + \sigma E_z) r^2 \tag{23}$$

Finally, the solution of Eq. (11) will be

$$T(r,z)=T_a+Az-\frac{E_z}{4k'}(\alpha' A+\sigma E_z)r^2 \tag{24}$$

Boundary condition (13) and relation (16) give

$$W_{R_c}=(-\beta E_z-k'A)U_z+\frac{E_z}{2}(\alpha' A+\sigma E_z)R_c Ur \tag{25}$$

From this relation the expression

$$A=\left[-\left(2\beta E_z k'+\frac{E_z^4\alpha'\sigma R_c^2}{2}\right)\Big/2\left(k'+\frac{E_z^2\alpha'^2}{4}\right)\right]$$
$$\pm\left\{\left[\left(2\beta E_z k'+\frac{E_z^4\alpha'\sigma R_c^2}{2}\right)\right]^2-4\left[-W_{R_c}+\beta^2 E_z^2\right.\right.$$
$$\left.\left.+\frac{E_z^4\sigma^2 R_c^2}{4}\right]\left(k'^2+\frac{E_z^2\alpha'^2}{4}\right)\right]^{1/2}\Big/2\left[k'+\frac{E_z\alpha'^2}{4}\right]\Bigg\} \tag{26}$$

is obtained.

The temperature must decrease with increasing z—then the negative value of A is taken. Also the condition

$$\alpha' A+\sigma E_z>0 \tag{27}$$

must exist, because the temperature decreases in the radial direction.

One may conclude that it is desirable in a cylindrical arc to make axial and radial temperature measurements in order to compare with the results from nonequilibrium thermodynamics modeling.

References

[1] Incropera, F. P., "Procedures for Modeling Lamianr Cascade Arc Behavior," *IEEE Transactions on Plasma Science*, Vol. PS-1, No. 3, 1973, p. 3.

[2] Elenbaas, W., *Physica*, Vol. 2, 1935, p. 169.

[3] Heller, G., *Physica*, Vol. 6, 1935, p. 359.

[4] Dresvin, S. V., ed., *Physics and Technology of Low-Temperature Plasmas*, English Ed., The Iowa State University Press, Ames, Iowa, 1977, pp. 284-298.

[5] Haines, M. G., *Plasma Physics, Lectures from the Culham Plasma Physics Summer Schools*, held at the UKAEA Culham Laboratory, Abingdon, edited by B. E. Keen, Conference Series No. 20, the Institute of Physics, London and Bristol, 1974, pp. 177-195.

[6] Shkarofsky, I. P., Johnston, T. W., and Bachinski, M. P., *The Particle Kinetics of Plasmas*, Addison-Wesley, 1966, p. 364.

[7] Fraley, S. K., Hoffman, T. J., and Stevens, P. N., "A Monte Carlo Method of Solving Heat Conduction Problems," *Journal of Heat Transfer*, Vol. 102, Feb. 1980, pp. 121-125.

Behavior of the Flow Through a Numerically Captured Shock Wave

David Nixon*

Nielsen Engineering & Research, Inc.

Mountain View, California

Introduction

At present the most common method of predicting transonic flow is to solve numerically the potential equation representing conservation of mass using a shock capturing algorithm.[1,2] In a shock capturing algorithm the shock is represented by a finite velocity gradient spread over several mesh points, rather than by a discontinuity. Two types of finite difference algorithms are in use: nonconservative algorithms which do not conserve mass through the shock wave and conservative algorithms which do conserve mass. The issue of conservation or nonconservation of mass through the shock wave concerns the end points of the shock capture region. This Note concerns the question of mass conservation during the shock capture in a conservative algorithm.

The conclusion of this analysis is that a conservative algorithm merely conserves mass at the end points of the shock capture region. In the shock region there is an increase in mass followed by a decrease in mass.

This work was initiated to assist in a related investigation[3]; however, it is felt that the analysis also is of some interest in aiding understanding of the numerical algorithms used in transonic flow predictions.

Received Nov. 30, 1982; revision received March 7, 1983.

Copyright © American Institute of Aeronautics and Astronautics, Inc., 1983. All rights reserved.

*Research Scientist. Associate Fellow AIAA.

Analysis

A simple description of transonic flow can be obtained by a study of the transonic small-disturbance equation, written in the form

$$[u-(u^2/2)]_x+v_y=0 \tag{1}$$

where $u=(\gamma+1)M_\infty^2/(1-M_\infty^2)(\partial\phi/\partial x)$, $v=(\gamma+1)M_\infty^2/(1-M_\infty^2)^{3/2}(\partial\phi/\partial y)$, and ϕ is the perturbation potential. In this formulation $u>1$ denotes a supersonic flow and $u<1$ denotes a subsonic flow. Equation (1) can give discontinuous solutions, which for a normal shock gives the jump relation

$$u_1+u_2=2 \tag{2}$$

It is usually the case that Eq. (1) is solved by a finite difference scheme with an artificial dissipation added in the supersonic domain by using an upwind difference procedure,[1,2] and in the following analysis it is assumed that upwind differencing is used throughout. One-dimensional examples have been computed[2] using this method.

The upwinding scheme of Murman[1] can be represented by a differential equation of the form that approximates Eq. (1) by

$$\frac{\partial}{\partial x}\left[\left(u-\frac{u^2}{2}\right)-\Delta x\left(u-\frac{u^2}{2}\right)_x\right]+v_y=0 \tag{3}$$

where Δx is the grid size. Equation (3) can be integrated to give

$$u-u^2/2=P(x,y)+C_2(y)e^{x/\Delta x} \tag{4}$$

where $V(x,y)$ is given by

$$V(x,y)=\int^x v_y \mathrm{d}x \tag{5}$$

where

$$P(x,y)=e^{x/\Delta x}\int^x [V(x,y)+C_1(y)]e^{-(x/\Delta x)}/\Delta x\mathrm{d}x \tag{6}$$

and $C_1(y)$ and $C_2(y)$ are arbitrary functions arising from the integration. $C_2(y)$ is also a function of Δx such that

$$\lim_{\Delta x\to 0} C_2(y)e^{x/\Delta x}\to 0$$

in order to recover the correct solution of Eq. (3) when $\Delta x=0$. If shock waves are normal to the x axis then V and C_1 are continuous functions of (x,y). Since $V(x,y)$, $C_1(y)$ are continuous functions, $P(x,y)$ is a continuous function; and since shocks are assumed normal to the x axis, $C_2(y)$ is a continuous function.